ISSN- 2230-7346
Journal of Global Trends in Pharmaceutical Sciences

FORMULATION AND ASSESMENT OF BIODEGRADABLE POLYMERIC ANTI-CANCER DRUG NANO PARTICLES

N. Audinaryana*, T. Sai Niharika, D. Jothieswari

Sri Venkateswara College of Pharmacy (Autonomous), RVS Nagar, Chittoor, 517127

*Corresponding author E-mail: **thallasainiharika@gmail.com**

ARTICLE INFO

Key words:

Anticancer, Gemcitabine, Pivarubicin, Double emulsion solvent evaporation.

Access this article online
Website: https://www.jgtps.com/
Quick Response Code:

ABSTRACT

The present study focuses on the design, synthesis, and comprehensive evaluation of PEG-PCL-based polymeric nanoparticles for the dual delivery of chemotherapeutic agents including Gemcitabine (GEM) and Pivarubicin (PIV), in combination with a MUC1 inhibitor, aimed at enhancing therapeutic efficacy through sustained and targeted release. Nanoparticles were prepared using a double emulsion solvent evaporation technique and were characterized for particle size, polydispersity index (PDI), zeta potential, and encapsulation efficiency (%EE). The single and dual drug-loaded nanoparticles exhibited high encapsulation efficiencies (85%–95%) and nanoscale sizes ranging from 64 nm to 129 nm. All formulations demonstrated narrow size distributions (PDI ≤ 0.088) and negative zeta potentials (up to –26.33 mV), indicating colloidal stability and uniformity. In vitro release studies conducted under physiological pH (7.4) over 60 days revealed a biphasic release pattern with an initial burst followed by a sustained release phase. Notably, the dual-loaded formulations (GM and DM NPs) showed synchronized and extended drug release, achieving 58%–65% cumulative release by day 60. These results confirm the successful co-encapsulation and controlled release of both cytotoxic and immunomodulatory agents from a single nanocarrier system. The developed nanosystems demonstrate promising potential as a combinatorial drug delivery platform for cancer therapy, offering improved bioavailability and prolonged therapeutic action.

INTRODUCTION

Biodegradable polymeric nanoparticles (BPNPs) represent a promising approach for targeted cancer therapy, offering improved drug delivery with reduced systemic toxicity. These nano-sized carriers enhance the efficacy of anticancer agents by protecting them from degradation, improving solubility, enabling controlled and stimuli-responsive release, and facilitating targeted delivery to tumors via passive and active mechanisms. Nanoparticles must navigate biological barriers, stabilize cargo, and enable intracellular or extracellular drug release, often in response to physiological triggers such as pH, temperature, or glutathione concentration.BPNPs can be formulated using natural polymers like chitosan and dextran, or synthetic polymers such as PLA, PLGA, PCL, and advanced materials like poly(β-amino esters) or stimuli-sensitive polymers. Methods of nanoparticle formation include self-assembly and emulsion techniques, yielding various structures like micelles, polyplexes, nanospheres, and nanocapsules. These formulations are tailored by modifying polymer composition, size, and surface properties to enhance biocompatibility, biodegradability, and drug-loading efficiency.By enabling localized delivery and lowering required dosages, polymeric nanoparticles minimize adverse effects

associated with conventional chemotherapeutics. Their tunability and versatility also support the delivery of both hydrophilic and hydrophobic drugs, including nucleic acids for gene therapy. As such, BPNPs are a key innovation in nanomedicine for more effective, safer cancer treatment.Polymeric nanoparticles, particularly those made from biodegradable polymers like PLA, PLGA, and PCL, are emerging as promising drug delivery systems in cancer therapy due to their biocompatibility, tunable degradation rates, and capacity for sustained and targeted drug release. These nanocarriers can encapsulate chemotherapeutic and peptide-based drugs, enhancing their stability, bioavailability, and tumor-specific delivery while reducing systemic toxicity. Several formulation methods are employed, including emulsification-solvent evaporation, nanoprecipitation, ionic gelation, and drying techniques. Surface functionalization (e.g., PEGylation) and targeting mechanisms (passive via EPR effect or active ligand-based) further enhance specificity and circulation time. The success of these systems depends on optimizing drug loading efficiency, polymer-drug compatibility, and controlled release mechanisms such as diffusion, degradation, and swelling. Characterization techniques like particle size analysis, zeta potential, SEM/TEM imaging, and in vitro drug release profiling are essential for evaluating nanoparticle quality. In vitro cytotoxicity assays (e.g., MTT, LDH), cell uptake studies, and in vivo pharmacokinetic and efficacy studies validate the therapeutic performance. Cancer remains a global health crisis, with millions of new cases and deaths each year. Traditional chemotherapy faces challenges including drug resistance, low tumor specificity, and high systemic toxicity. Nanoparticle-based drug delivery systems can address these limitations by improving tumor targeting and reducing off-target effects. Moreover, combination therapy involving both chemotherapeutics and peptide-based agents within a single nanoparticle can potentially enhance efficacy while minimizing side effects and overcoming multidrug resistance. Despite their advantages, challenges such as scalability, batch variability, regulatory approval, and tumor heterogeneity must be addressed. Nonetheless, polymeric nanoparticles represent a transformative strategy for next-generation cancer therapy with the potential to significantly improve patient outcomes.Chemotherapy is a common cancer treatment that uses drugs to kill fast-growing cancer cells, but it can also harm healthy cells, causing side effects like nausea, hair loss, and mouth sores. Chemotherapeutic agents are classified into groups based on their action, such as alkylating agents, antimetabolites, antitumor antibiotics, topoisomerase inhibitors, mitotic inhibitors, and corticosteroids. To reduce toxicity and improve specificity, biomolecules like nucleic acids, proteins, and peptides are being explored for targeted cancer therapy. Nanotechnology has emerged as a promising tool in cancer treatment by allowing the precise delivery of drugs using nanoparticles (NPs), which improve drug stability, reduce side effects, and increase accumulation in tumors. Liposomes and polymeric nanoparticles like PLGA and PEG-PLGA are widely used for drug delivery, often modified with targeting molecules such as peptides or aptamers. These nanocarriers have shown enhanced effectiveness in killing cancer cells and overcoming drug resistance. Combination therapy using multiple drugs loaded into a single nanocarrier helps lower individual drug doses, reduce toxicity, and prevent cancer relapse. Advanced carriers like calcium phosphate and mesoporous silica nanoparticles offer controlled drug release and better bioavailability. Despite challenges like formulation complexity and regulatory barriers, nanotechnology continues to play a key role in advancing safer, more effective cancer therapies. Polymer-based nanocarriers have shown significant promise in both preclinical and clinical cancer therapies due to their ability to improve drug delivery through passive and active targeting strategies. These systems enhance drug accumulation at tumor sites via the enhanced permeability and retention (EPR) effect and can be further modified with targeting ligands for specific cellular uptake. Polymeric micelles formed from amphiphilic block copolymers offer stable drug loading and prolonged circulation. To treat challenging cancers like glioblastoma, nanocarriers can be locally administered during surgery to deliver therapeutic genes,

enabling site-specific drug activation and reducing toxicity to healthy tissue. Biodegradable polymers are engineered for both passive targetingleveraging leaky tumor vasculature—and active targeting by attaching ligands that bind to cancer-specific surface molecules, triggering cellular uptake. Moreover, these nanocarriers support angiogenesis modulation and immune engineering approaches by delivering vaccines, genes, or artificial antigen-presenting cells, thus enabling precise control over immune responses. Overall, polymeric nanocarriers offer a versatile and effective platform for targeted cancer therapy, but safety and delivery across biological barriers remain crucial considerations for clinical application.

2. MATERIALS:

All chemicals used in the study were of analytical grade and procured from commercial sources. Polyethylene glycol (PEG, Mn = 5,000 Da), ε-caprolactone (purity ≥ 95%), phosphate-buffered saline (PBS), Coumarin-6, Rhodamine B, and other related salts were obtained from Sigma-Aldrich and Merck.

2.1 Synthesis of PEG-PCL copolymer synthesis: Methoxy poly(ethylene glycol) (MPEG, Mn = 5000 Da) was subjected to azeotropic dehydration with toluene under reflux for 6 hours to eliminate residual moisture. Subsequently, MPEG was combined with ε-caprolactone (ε-CL), previously activated by stirring over molecular sieves for 24 hours, and the mixture was magnetically stirred to ensure homogeneity.The ring-opening polymerization reaction was conducted in a dry, nitrogen-purged round-bottom flask connected to a vacuum system. MPEG served as the macroinitiator, and stannous octoate ($Sn(Oct)_2$) was employed as the catalyst. The polymerization was carried out at 120 °C under reduced pressure for 24 hours.Upon completion, the reaction mixture was cooled to ambient temperature and subjected to multiple precipitations in cold, anhydrous diethyl ether to remove residual monomers and low molecular weight oligomers. The resultant polymer was collected by filtration and dried under vacuum at 40 °C for 24 hours. The purified PEG-PCL block copolymer was stored in a desiccator until further use.

3. METHODOLOGY:

Nanoparticles were formulated using the double emulsion (water-in-oil-in-water, W/O/W) solvent evaporation technique employing PEG-PCL as the biodegradable copolymer matrix. For the organic phase, PEG-PCL copolymer along with the hydrophobic drug Pivarubicin was dissolved in dichloromethane (DCM), while the hydrophilic drugs including Gemcitabine and the MUC1 inhibitorwere dissolved separately in distilled water to constitute the internal aqueous phase. The aqueous drug solution was added dropwise into the organic phase under continuous magnetic stirring, followed by probe sonication to form a stable primary W/O emulsion. This primary emulsion was then slowly added to an external aqueous phase containing 1–2% w/v polyvinyl alcohol (PVA) under further sonication to generate the secondary W/O/W double emulsion. The resulting emulsion was stirred at 37 ± 5 °C for 4–6 hours to ensure complete evaporation of the organic solvent, facilitating nanoparticle hardening. Nanoparticles were harvested via centrifugation at 10,000 rpm for 10 minutes at 4 °C, washed thrice with distilled water to eliminate residual PVA and unencapsulated drug, and finally resuspended in a 5% w/v trehalose solution. The dispersion was then subjected to freeze-drying (lyophilization) to obtain a dry, free-flowing nanoparticulate powder suitable for long-term storage. This method ensured efficient encapsulation of both single and dual therapeutic agents within the PEG-PCL matrix, enhancing their stability and potential for controlled release.

3.1 Construction of calibration curve:

To construct a calibration curve for drug quantification, a series of standard solutions of the pure drug (e.g., Gemcitabine) were prepared using phosphate buffer (pH 7.4) as the solvent. A stock solution was initially prepared by dissolving 10 mg of the drug in 10 mL of buffer to obtain a concentration of 1 mg/mL (1000 µg/mL). From this stock, serial dilutions were made to yield working standards in the range of 5–30 µg/mL. The absorbance of each standard solution was measured at the drug's maximum absorbance wavelength (λmax), which was approximately 268 nm for Gemcitabine, using a UV-Visible spectrophotometer. A calibration curve was

generated by plotting absorbance against drug concentration, and linear regression analysis was performed to obtain the calibration equation. The resulting plot demonstrated excellent linearity with a correlation coefficient (R^2) greater than 0.99, confirming the reliability of the method for quantitative analysis. This calibration curve was subsequently used to determine the drug content and entrapment efficiency in the nanoparticle formulations.

3.2 Synthesis of Nanoparticles:

PEG-PCL nanoparticles (NPs) were prepared using a modified double emulsion (water-in-oil-in-water, W/O/W) solvent evaporation technique for the encapsulation of hydrophilic and hydrophobic anticancer agents Gemcitabine (GEM), Pivarubicin (PIV) either alone or in combination with a MUC1 inhibitor. Initially, 100 mg of the synthesized PEG-PCL di block copolymer was dissolved in 5 mL of acetonitrile to form the organic phase. For single-drug formulations, 10 mg of either GEM or PIV was added to the organic phase and sonicated briefly (30 seconds at 20% amplitude) using a probe sonicator to ensure homogeneous dispersion. For dual-drug-loaded nanoparticles, an appropriate amount of MUC1 inhibitor was co-dissolved or co-emulsified based on its solubility profile (hydrophilic or lipophilic). The resulting primary emulsion (W/O) was formed by emulsifying the drug-polymer solution with 1 mL of aqueous drug solution or buffer containing hydrophilic agents, followed by probe sonication (30 seconds on/30 seconds off, 3 cycles) in an ice bath to prevent thermal degradation. This primary emulsion was then added dropwise into 25 mL of an aqueous phase containing 1% (w/v) Poloxamer 407 (F127) under continuous magnetic stirring at 800 rpm. The emulsion was stirred at room temperature for 24 hours to allow complete solvent evaporation and nanoparticle formation. Post-evaporation, the nanoparticles were collected and purified by ultrafiltration using a 10 kDaAmicon® Ultra centrifugal filter unit (Millipore, USA) at 4000 rpm for 20 minutes to remove unencapsulated drug and free polymer. The purified nanoparticles were washed with deionized water and subsequently lyophilized using a laboratory freeze-dryer (Christ Alpha 1–2 LD plus) after pre-freezing at −80 °C for 12 hours. The lyophilized nanoparticles were stored at −20 °C in airtight vials until further use.

4. CHARACTERIZATION STUDIES:

4.1 Characterization of PEG-PCL copolymer

4.1.1 Fourier Transform Infra-Red Spectroscopy (FTIR):

FTIR spectroscopy was utilized to investigate the structural characteristics and functional group composition of the synthesized polymer. This technique enables the identification of organic, inorganic, and polymeric substances by detecting their unique vibrational transitions upon interaction with infrared radiation. Changes in the absorption profile correspond to variations in chemical bonding and molecular structure, allowing for qualitative assessment of copolymer formation, detection of impurities, and monitoring of degradation or oxidation processes. For analysis, the polymer sample was cast into a thin film by solvent evaporation and subsequently mounted on a sodium chloride (NaCl) crystal plate. The infrared absorption spectrum was recorded over the range of 4000 to 400 cm^{-1} using an RZX model FTIR spectrometer (Perkin Elmer, UK). This spectral data facilitated the confirmation of successful copolymerization by identifying characteristic functional groups associated with both PEG and PCL segments.

Encapsulation efficacy:

The encapsulation efficacy was determined by quantifying the free drug separated from the nanoparticle suspension after the synthesis. A known quantity of the nanoparticle formulation was subjected to ultrafiltration using Amicon® Ultra centrifugal filter units (10 kDa molecular weight cut-off) at 4000–8000 rpm for 15–30 minutes. The filtrate containing the drug was analyzed using UV-Visible spectrophotometry and for the determination of the total drug content, a known quantity of the nanoparticles are dissolved in the suitable solvent such as DMSO, acetonitrile or methanol and quantified using the method described above.

$$\text{Encapsulation efficacy} = \frac{\text{Total drug added-Free drug detected}}{\text{Total drug added}} \times 100$$

Similarly, the drug loading capacity was estimated by using the formula:

$$\text{Drug Loading} = \frac{\text{Encaosulated drug}}{\text{Total weight of the nanoparticles}} \times 100$$

Particle size determination:

The average particle size and size distribution of the synthesized nanoparticles were analyzed using dynamic light scattering (DLS) with a NanoSight NS500 (UK). DLS measures particle size based on the Brownian motion of particles in suspension. The hydrodynamic diameter is calculated using the Stokes-Einstein equation. This method provides insights into nanoparticle uniformity and colloidal stability. All measurements were performed at 25 °C in triplicate using freshly prepared, diluted nanoparticle suspensions.

Determination of Zeta potential:

Zeta potential of the nanoparticles was measured using electrophoretic light scattering (ELS) to evaluate their colloidal stability. Upon application of an electric field, charged particles in suspension migrate toward the oppositely charged electrode, with their velocity determined by the balance between electrostatic and viscous forces. The electrophoretic mobility was converted to zeta potential using the Smoluchowski equation. Measurements were performed in phosphate-buffered saline (PBS, pH 7.4) to simulate physiological conditions and assess nanoparticle stability under biologically relevant ionic strength.

Drug release studies:

The in vitro release profile of Gemcitabine, Pivarubicin, and the MUC1 inhibitor from PEG-PCL-based nanocarriers was assessed using a centrifugal ultrafiltration method under physiologically relevant conditions. Precisely 20 mg of lyophilized nanoparticles were reconstituted in phosphate-buffered saline (PBS, pH 7.4) and incubated at 37 °C with mild orbital agitation (100 rpm) to simulate systemic circulation. At predefined time intervals over a 60-day release period, aliquots were withdrawn and subjected to centrifugal filtration using 10 kDa molecular weight cut-off Amicon® Ultra centrifugal devices (Millipore) to selectively isolate the released drug fraction from the nanoparticulate matrix. Following each collection, fresh PBS was added to maintain constant volume and preserve sink conditions. Quantitative analysis of Gemcitabine and Pivarubicin concentrations in the filtrates was conducted using high-performance liquid chromatography (HPLC), while the MUC1 inhibitor levels were determined via a Micro-BCA protein assay. All measurements were performed in triplicate, and cumulative drug release was expressed as a function of time to evaluate sustained release kinetics.

5. RESULTS AND DISCUSSION:

FTIR Studies:

The FTIR spectrum of the synthesized PEG-PCL copolymer confirms successful copolymerization through characteristic vibrational peaks. A broad peak at 3452.34 cm^{-1} corresponds to O–H stretching, indicating terminal hydroxyl groups or moisture. Peaks at 2885.37 cm^{-1} and 2698.06 cm^{-1} are attributed to C–H stretching of methylene ($–CH_2$) groups. The sharp band at 1724.57 cm^{-1} is indicative of ester carbonyl (C=O) stretching, confirming ring-opening polymerization of ε-caprolactone. Absorptions at 1466.07 cm^{-1} and 1359.45 cm^{-1} represent $–CH_2$ bending vibrations. The peak at 1102.98 cm^{-1} corresponds to C–O–C stretching, characteristic of PEG ether linkages. Additional bands at 1240.25 cm^{-1} and 1174.21 cm^{-1} reflect ester C–O vibrations from the PCL segment. Minor peaks between 800 and 700 cm^{-1} are attributed to out-of-plane C–H bending (Figure 1). These results confirm the structural integrity and successful synthesis of PEG-PCL copolymer. Spectral assignments are consistent with previously reported literature values.

Dynamic Light Scattering (DLS) and Zeta potential:

Dynamic Light Scattering (DLS) was employed to evaluate the hydrodynamic diameter and colloidal stability of the synthesized nanoparticles by measuring their Brownian motion and corresponding zeta potential. As detailed in Table 1, the mean particle size of blank nanoparticles was approximately 64 nm. Upon individual encapsulation with Gemcitabine and the MUC1 inhibitor, the particle sizes increased to 93.33 nm and 95 nm, respectively, indicating successful drug loading. The dual drug-loaded

formulation (Gemcitabine + MUC1 inhibitor) exhibited a further size increment to 128.66 nm, likely due to increased core content and polymer matrix swelling. Similarly, in the Pivarubicin-loaded series, the particle sizes increased to 94 nm and 95 nm upon incorporation of Pivarubicin and MUC1 inhibitor, respectively (Table 2). All nanoparticle formulations demonstrated negative zeta potential values, indicative of strong electrostatic repulsion among particles and enhanced colloidal stability. The observed increase in size for dual drug-loaded nanoparticles correlates with higher drug payloads, which may contribute to a more prolonged and controlled drug release profile.

Encapsulation efficacy of Nanoparticles:

The single drug-loaded nanoparticle formulations exhibited high encapsulation efficiencies, confirming the effective entrapment of therapeutic agents within the PEG-PCL polymeric matrix. Specifically, Gemcitabine-loaded nanoparticles (GEM NPs) achieved an encapsulation efficiency (EE) of85.4%**,** while MUC1 inhibitor-loaded nanoparticles (MUC1 NPs) demonstrated an EE of 95%**,** indicating robust drug-polymer interaction and minimal drug loss during formulation. The dual-loaded system (GM NPs), co-encapsulating both Gemcitabine and the MUC1 inhibitor, preserved high encapsulation efficiencies of 85.05% and 89.05%**,** respectively, highlighting the formulation's capacity for simultaneous incorporation of multiple therapeutic agents without compromising individual drug entrapment (Table 1). Similarly, the Pivarubicin-loaded formulation (PIV NPs) exhibited an EE of 85.5%**,** and the corresponding dual drug-loaded system (DM NPs), comprising both Pivarubicin and MUC1 inhibitor, achieved encapsulation efficiencies of 86.8% and 89.25%**,** respectively (Table 2). These results collectively underscore the efficiency of the PEG-PCL nanoparticle platform in encapsulating both single and dual drug combinations, supporting its potential for combination therapy applications.

Particle Size:

The baseline hydrodynamic diameter of the blank PEG-PCL nanoparticles was recorded as 64 ± 18 nm, representing the unloaded polymeric carrier system. A significant increase in particle size was observed following drug incorporation, confirming successful encapsulation and interaction between the polymer and active agents. In the case of Gemcitabine-loaded and MUC1 inhibitor-loaded nanoparticles, the average particle sizes increased to 93.33 ± 9.6 nm and 95 ± 12.5 nm, respectively. The dual drug-loaded formulation (GM NPs), encapsulating both Gemcitabine and the MUC1 inhibitor, showed a further size enlargement to 128.66 ± 23 nm**,** which can be attributed to the increased molecular payload and potential polymer matrix expansion (Table 1). Conversely, in the Pivarubicin series, individual loading of MUC1 inhibitor resulted in a particle size of 95 ± 12.5 nm, while the dual-loaded nanoparticles (DM NPs), containing both Pivarubicin and MUC1 inhibitor, exhibited a slightly smaller size of 93.33 ± 9.6 nm (Table 2). This reduction may be due to a more compact internal arrangement or synergistic interactions between the encapsulated agents, promoting tighter packing within the nanoparticle core. Overall, the variations in particle size reflect the influence of drug composition and loading strategy on nanoparticle architecture.

Zeta Potential:

All nanoparticle formulations exhibited negative zeta potential values, indicative of favorable colloidal stability arising from electrostatic repulsion between particles. The blank PEG-PCL nanoparticles displayed a baseline zeta potential of -13.5 ± 2.5 mV. Upon drug loading, a shift toward more negative surface charges was observed. Specifically, MUC1 inhibitor-loaded NPs demonstrated a zeta potential of -20.26 ± 1.9 mV, while Gemcitabine-loaded NPs (GEM NPs**)** exhibited a further increase in negativity to -26.33 ± 0.27 mV, likely due to ionizable groups present in the encapsulated drug interacting with the nanoparticle surface. In contrast, the dual-loaded formulation (GM NPs) showed a reduction in zeta potential to -10.66 ± 1.28 mV, which could be attributed to surface shielding effects or rearrangement of surface functional groups resulting from the co-encapsulation of both drugs (Table 1). Similarly, in the Pivarubicin series, PIV NPs and MUC1 NPs maintained negative zeta potentials of -22.33 ± 1.5 mV and –

20.26 ± 1.9 mV, respectively (Table 2). However, the dual-loaded DM NPs exhibited a markedly less negative zeta potential of –1.6 ± 2.5 mV, suggesting potential masking of surface charges or alterations in the interfacial characteristics due to the combined drug payload. These variations in surface charge highlight the influence of drug composition on nanoparticle interface properties and may have implications for in vivo stability, biodistribution, and cellular interaction.

Polydispersity Index:

All synthesized nanoparticle formulations demonstrated low polydispersity index (PDI) values, reflecting a high degree of uniformity in particle size distribution and indicating successful formulation of monodisperse systems. Specifically, the blank nanoparticles exhibited a PDI of 0.079, while MUC1 inhibitor-loaded NPs showed a more uniform distribution with a PDI of 0.017. Among the drug-loaded systems, the Gemcitabine-loaded NPs (GEM NPs) and dual-loaded GMNP**s** maintained a highly monodisperse profile, both recording a PDI of 0.010, suggesting that the inclusion of multiple therapeutic agents did not adversely affect nanoparticle uniformity (Table 1). In the Pivarubicin group, PIV NPs displayed a slightly broader distribution with a PDI of **0.088**, though still within acceptable limits for nanoparticulate systems. Notably, the dual-loaded DM NPs also exhibited a PDI of 0.010, confirming the ability of the PEG-PCL matrix to maintain size homogeneity even under dual drug loading conditions (Table 2). Collectively, these results highlight the robustness of the formulation method in generating nanoparticles with consistent size characteristics, which is critical for reproducibility, biodistribution, and drug release performance.

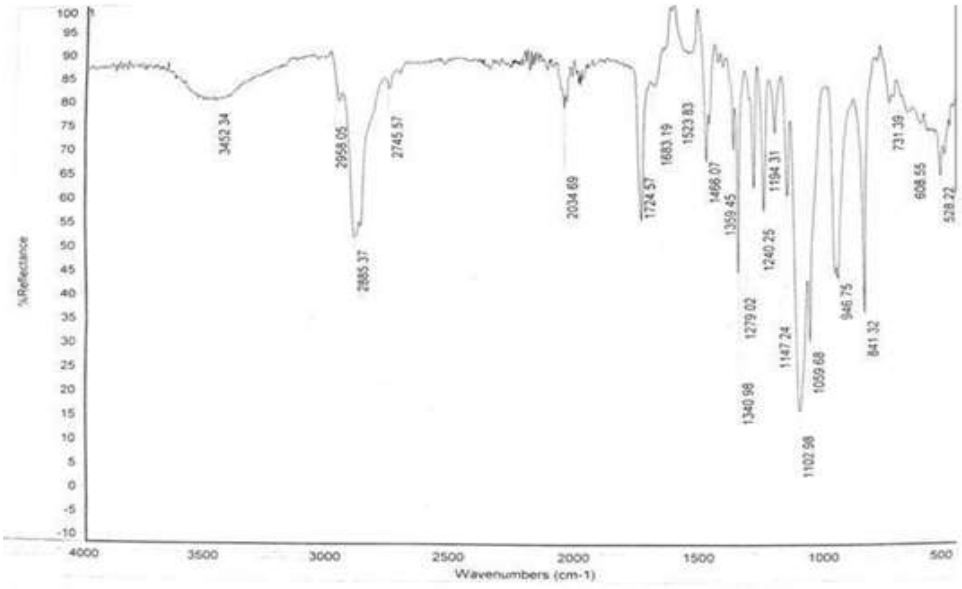

Figure 1: FTIR spectrum of PEG–PCLdiblockcopolymer

Table1: Diblock NPs encapsulating GEM physico-chemical characteristics alone or in combination with MUC1 inhibitor

Nano Particles	GEM/ MUC1	Drug/ Polymer	% EE (MUC1)	% EE	Size (nm)	Zeta Potential	PDI
Blank					64±18	-13.5±2.5	0.079
MUC1	0:1	1:10		93.3	95 ±12.5	-20.26±1.9	0.017
GEM NPs	1:0	1:10	85.4		93.33±9.6	-26.33±0.27	0.010
GM NPs	1:1	1:10	85.05	89.05	128.66±23	-10.66 ±1.28	0.010

Table 2: Diblock NPs encapsulating PIV physio-chemical characteristics alone or incombination with MUC1 inhibitor

Nano Particles	GEM/ MUC1	Drug/ Polymer	% EE (MUC1)	% EE	Size (nm)	Zeta Potential	PDI
Blank					64±18	-13.5±2.5	0.079
MUC1	0:1	1:10		93.3	95 ±12.5	-20.26±1.9	0.017
PIV NPs	1:0	1:10	85.5			-22.33±1.5	0.088
DM NPs	1:1	1:10	86.8	89.25	93.33±9.6	-1.6±2.5	0.010

***In-vitro* drug release studies:**

The release dynamics of GEM), PIV, and the MUC1 inhibitor from their respective nanoparticulate delivery systems were systematically investigated under physiological pH conditions (7.4) for a duration of 60 days. GEM-loaded nanoparticles (GEM NPs) exhibited an initial burst release phase (11%/day), followed by a sustained release profile ranging from 1% to 3% daily, culminating in a cumulative release of approximately 48% within the first 10 days. MUC1 inhibitor-loaded nanoparticles (MUC1i NPs) displayed an analogous biphasic release pattern. Co-encapsulated GEM–MUC1i nanoparticles (GM NPs) demonstrated cumulative 10-day release values of 45% for GEM and 50% for the MUC1 inhibitor. The daily release kinetics of GEM from GM NPs remained comparable to that of GEM NPs, while the MUC1 inhibitor exhibited a moderately attenuated release rate relative to MUC1i NPs. Likewise, PIV-loaded nanoparticles (PIV NPs) showed a 49% cumulative release over 10 days, with an initial burst of ~10% followed by a controlled release phase of 1–2.5% per day. Dual-loaded PIV–MUC1i nanoparticles (DM NPs) achieved co-release values of 43% (PIV) and 49% (MUC1 inhibitor) at day 10, increasing to 58% and 65%, respectively, by day 60. The release profile of PIV from DM NPs mirrored that of the single-loaded PIV NPs, whereas MUC1 inhibitor release was comparatively slower than from MUC1i NPs. These release profiles validate the successful co-entrapment of chemotherapeutics and MUC1 inhibitor within a single nanocarrier system, with the dual-loaded GM and DM NPs effectively sustaining controlled and prolonged drug release kinetics.

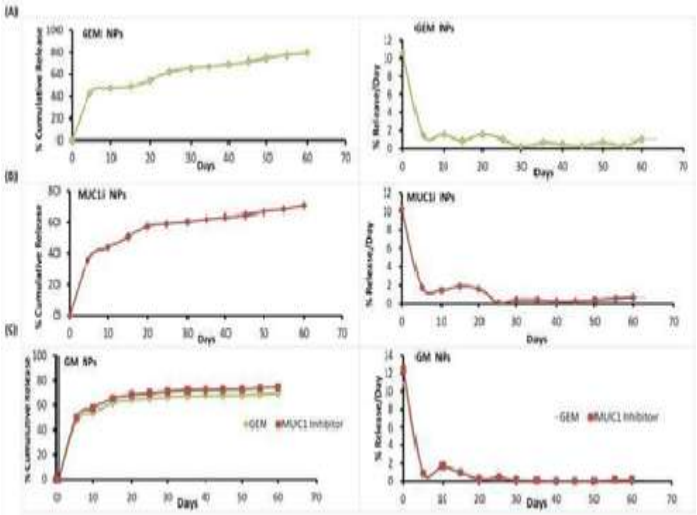

Figure 2: *In-vitro* drug releases study of GEM and MUC1 Inhibitor from PEG-PCLNPs.

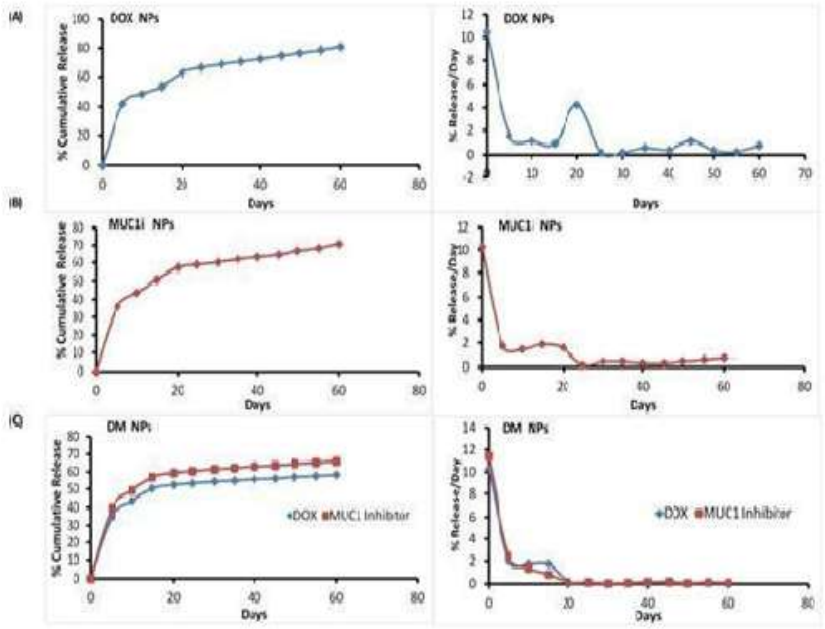

Figure 3: *In-vitro* drug releases study of PIV and MUC1 Inhibitor from PEG-PCLNPs

CONCLUSION:

The present invention relates to the development and characterization of PEG-PCL-based nanoparticulate drug delivery systems for the co-delivery of chemotherapeutic agentsGEM and PIValongside a MUC1 inhibitor, with the goal of achieving sustained and controlled release under physiological conditions. The nanoparticles were synthesized via the double emulsion (W/O/W) solvent evaporation method, and characterized in terms of encapsulation efficiency (EE), particlesize, zeta potential, and PDI. High EE values were obtained for both single and dual drug-loaded formulations (ranging from 85% to 95%), confirming efficient entrapment within the PEG-PCL matrix. Particle size analysis revealed nanoscale dimensions with significant size increases upon drug loading, particularly for dual-loaded systems (GM NPs: 128.66 nm; DM NPs: 93.33 nm), while all formulations maintained low PDI values (≤0.088), indicating monodispersity. Zeta potential measurements demonstrated negative surface charges across all formulations, suggesting favorable colloidal stability due to electrostatic Repulsion. *In vitro* drug release studies conducted at pH 7.4 over a 60-day period revealed biphasic release kinetics for all formulations. GEM NPs exhibited an initial burst release (~11% per day), transitioning to a sustained phase (1–3% daily), reaching ~48% cumulative release by day 10. Similarly, MUC1i NPs displayed a biphasic pattern, while co-loaded GM NPs released 45% of GEM and 50% of the MUC1 inhibitor within the same timeframe. The release rate of GEM from GM NPs paralleled that of the single-loaded system, whereas the MUC1 inhibitor showed a slightly attenuated profile. PIV NPs also demonstrated biphasic kinetics with a 49% release at day 10, and DM NPs achieved co-release values of 43% (PIV) and 49% (MUC1 inhibitor), which extended to 58% and 65% respectively by day 60. These findings confirm the successful co-encapsulation and synchronized release of chemotherapeutic agents and immunomodulatory inhibitors from a single nanocarrier, supporting the platform's potential for enhanced therapeutic efficacy through sustained dual-drug delivery.

REFERENCES:

1. Abshire Dand LangMK (2018).The Evolution of Radiation Therapy in Treating Cancer. *Semin. Oncol. Nurs*. 34(2):151-157.
2. Gogoi M, Kumar N, Patra S (2016). Multifunctional magnetic liposomes for cancer imaging and therapeutic applications.In:HolbanA.M.,Grumezes cu G.,editors.*NanoarchitectonicsSmart DeliveryDrug Targeting.* Elsevier; Amsterdam, The Netherlands:pp. 743–782.
3. Hafeez U,GanHK, Scott AM (2018). Monoclonal antibodiesas immune modulatory therapy gainst cancer and auto immunediseases.*CurrOpinPharmacol*. 41:114-121
4. Ahmad R, Raina D, Trivedi V, Kawano T, RenJ, Kharbanda S, et al.(2007). MUC1 oncoprotein activates the IkappaB kinase βcomplex and constitutiveNF- kappaB signaling. *Nat Cell Biol.* 9:1419–27.
5. Jain AK, Swarnakar NK, Godugu C, Singh RP, Jain S (2011). The effect of the oral administration of polymeric nanoparticles on the efficacy and toxicity of tamoxifen. *Biomaterials.* 32(2):503–515.
6. LiJ,Yang, Bertino A ,GlaspyJ,Roberts Thrombocytopenia caused by the development thrombopoietin. *Blood*. 98(12): 3241-3248.
7. Muthu MS, formulations of risperidone: preparation evaluation *Nanomedicine*.5 (3):323-33. (2009). PLGA nanoparticle and neuropharmacological
8. Oyewumi MO,Yokel RA,Jay M,Coakley T,MumperRJ(2004).Comparison of cell uptake, biodistribution and tumor retention of folate-coated and PEG-coated gadolinium nanoparticle sintumor-bearing mice.*J.Control Release.* 95:613–626
9. PetreCE and Dittme rDP(2007).Liposomal daunorubicina streatment for Kaposi's sarcoma. *Int. J. Nanomed.* 2:277–288.
10. Ramasamy S, Duraisamy S, Barbashov S, Kawano T, Kharbanda S, KufeD(2007). The MUC1 and galectin-3 oncoproteins function in a microRNA- dependent regulatory loop. *Mol Cell.* 27:992–1004.
11. SafraT(2003).Cardiac Safety of Liposomal Anthracyclines.*Oncologist.*8:17–24.
12. Tancini B, TosiG, BortotB, DolcettaD, MaginiA, De MartinoE, etal. (2015).Use of polylactide-co-glycolide-nanoparticles for lysosomal delivery of a therapeutic enzyme in glycogenosis typeII fibroblasts.*J. Nanosci. Nanotechnol.* 15:2657–2666.
13. WalyMI and Rahman MS(2018).Bioactive Components, Diet and Medical Treatment in Cancer Prevention. ISBN : 978-3-319-75692-9
14. VhoraI,PatilS, BhattP, MisraA.(2015).Protein–and Peptide–Drug Conjugates: An Emerging Drug Delivery Technology. *In Advances in Protein Chemistry and Structural Biology;Rossen,D.,Ed.;AcademicPress Elsevier: Cambridge, MA, USA*. 98:1–55.
15. Ulbrich, Holá K,(2016). Targeted Drug Delivery with Polymers and Magnetic Nanoparticles: Covalent and Noncovalent Approaches, Release Control,and Clinical Studies.*Chem. Rev.* 116:5338–5431
16. Torchilin V P (2005). Recent advances with liposomes as pharmaceutical carriers. *Nat. Rev. Drug Discov.* 4:145–160
17. XuJL,Jin B,Ren ZH,LouYQ, ZhouZR,YangQZ,etal.(2015). Chemotherapy plus Erlotinib versus Chemotherapy Alone for Treating Advanced Non-Small Cell Lung Cancer: A Meta-Analysis. *PLoS ONE.* 10:e0131278.
18. Yordanov G,SkrobanskaR, EvangelatovA(2012).Entrapment of epirubicin in poly(butyl cyanoacrylate) colloidal nanospheres by

nanoprecipitation: formulationdevelopmentandinvitrostudiesoncancercelllines.*Colloids Surf B Biointerfaces.* 92:98–105.
19. ZhangZ,XiongX,WanJ,XiaoL,GanL,FengY,XuH,YangX
20. (2012).Cellular uptake and intracellular trafficking of PEG-b-PLA polymeric micelles. *Biomaterials.* 33:7233–7240.
21. Zielinski C, Beslija S, Mrsic-Krmpotic Z, Welnicka-Jaskiewicz M, Wiltschke C, Kahan Z, et al. (2005). Gemcitabine, epirubicin, and paclitaxel versus fluorouracil, epirubicin, and cyclophosphamide as first-line chemotherapy in metastatic breast cancer: a Central European Cooperative Oncology Group International, multicenter, prospective,randomized phase IIItrial. *J.Clin. Oncol.* 23:1401–1408.
22. WesselingJ,vanderValkSW,VosHL,SonnenbergA, HilkensJ (1995). Episialin (MUC1) over expression inhibits integrin-mediated celladhesion to extracellular matrix components. *J. Cell Biol.* 129: 255–265
23. RoyPS and SaikiaBJ(2016).Cancer and cure:A critical analysis.*Indian J.Cancer.*53(3): 441-442.
24. PiaoL,DaiZ, DengM, ChenX, JingX(2003).Synthesis and characterization of PCL/PEG/PCL triblockcopolymersbyusingcalciumcatalyst.*Polymer*.44(7): 2025-2031.
25. Moreno D, Zalba S, Navarro I, Tros de Ilarduya C, Garrido MJ (2010). Pharmacodynamics of cisplatin-loaded PLGA nanoparticles administered to tumor-bearing mice. *Eur. J. Pharm. Biopharm.* 74(2):265–274.
26. Kris R M, Lax I,Gullick,etal. (1985).Antibodiesagainstasyntheticpeptideasaprobeforthekinase activity of the avian EGF receptor and verbB protein. *Cell* .40(3): 619–25.
27. Hoang NH, Lim C, Sim T, Oh KT (2017). Triblock copolymers for nano-sized drug delivery systems. *J. Pharm. Investigation.* 47:27-35
28. Gryparis EC, Hatziapostolou M, Papadimitriou E, Avgoustakis K (2007). Anticanceractivityofcisplatin-loadedPLGA-mPEGnanoparticleson LNCaP prostate cancer cells. *Eur. J. Pharm. Biopharm.* 67(1):1–8.
29. FarokhzadOCandLangerR(2009).Impactofnanotechnologyondrugdelivery.*ACSNano.* 3:16–20
30. Duan X,ChanC, NiningGuo, W Han,WeichselbaumR R,LinW (2016). Photodynamic Therapy Mediated by Nontoxic Core-Shell Nanoparticles Synergizes with Immune Checkpoint Blockade To Elicit Antitumor Immunity and Antimetastatic Effect on Breast Cancer. *J. Am. Chem. Soc*. 138(51):16686-16695.
31. CristianoMC,CoscoD,CeliaC,TudoseA,MareR,PaolinoD,et al.(2017). Anticancer activity of all-trans retinoic acid-loaded liposomes on human thyroid carcinoma cells. *Colloids Surf. B: Biointerfaces.* 150:408–416.
32. AlfurhoodJA,SunH,KabbCP,TuckerBS,MatthewsJH,LueschH,et al.(2017). Poly(N-(2 hydroxypropyl) methacrylamide)-valproic acid conjugates as block copolymer nanocarriers. *Polym. Chem.* 8:4983–4987.
33. Behzadi S,Serpooshan V, Tao W,Hamaly MA Alkawareek MY,Dreaden EC, et al.(2017). Cellular uptake of nanoparticles: Journey inside the cell. *Chem. Soc. Rev.*46:4218–4244.
34. CavalliR,Bisazza A,BussanoR, TrottaM,Civra A,LemboD,etal. (2011). Poly(amidoamine)-cholesterol conjugate nanoparticles obtained by electrospraying as novel tamoxifen delivery system. *J Drug Deliv.* 2011:587604.
35. FangJ,Nakamura H,MaedaH (2011).The EPReffect: Unique featureso f tumor blood vessels for drug delivery, factors involved,and limitations and augmentation of the effect. *Adv. Drug Deliv. Rev.* 63(3):136-151.

36. GiljohannandDA and MirkinCA(2009).Drivers of biodiagnostic development. *Nature.* 462:461–464.
37. HanahanD and Weinberg RA(2011).Hallmarks of cancer:the next generation. *Cell.*144:646–674.
38. Jones C M, Pierre K B, Nicoud I B, Stain S C, Melvin W V (2006) Electrosurgery. *Curr. Surg* .63(6):458-63.
39. Kim MS, Seo KS, Khang G, Cho SH, Lee HB (2004). Preparation of poly(ethylene glycol)-block-poly(caprolactone)copolymers and their applications as thermo-sensitive materials. *J. Biomed. Mater. Res. A.* 70(1):154-8
40. Leng Y,Cao C, Ren J, Huang L,Chen D,Itoet Metal. (2007). Nuclear import of the MUC1-C oncoprotein is mediated by nucleoporin Nup62. *J Biol Chem.*282:19321–30.
41. PérezE, Benito M, TeijónC, Olmo R, Teijón JM, Blanco MD(2012). Tamoxifen loaded nanoparticles based on a novel mixture of biodegradable polyesters: characterization and in vitro evaluation as sustained release systems. *J. Microencapsul.* 29(4):309–322.
42. Rondeau V, Mathoulin-Pélissier S, Tanneau L, Sasco AJ, Macgrogan G, Debled M(2010).Separate and combined analysis of successive dependent outcomes after breast conservation surgery: recurrence, metastases, secondcancer and death. *BMC Cancer*. 2010;10:697.
43. Sharma S,GuruSK, MandaS,KumarA, Mintoo MJ, PrasadVD, etal.(2017). Amarinesponge alkaloid derivative4-chlorofascaplysin inhibits tumor growth and VEGF mediated angiogenesis by disrupting PI3K/Akt/mTOR signaling cascade. *Chem. Biol. Interact.* 275:47-60
44. Takebe N, Miele L, Harris PJ, Jeong W, Bando H, Kahn M, et al. (2015). Targeting Notch, Hedgehog, and Wnt pathways in cancer stem cells: clinical update. *Nat. Rev. Clin. Oncol.* 12:445-64.
45. Wang-GillamA, LiCP,BodokyG, DeanA,ShanYS ,JamesonG,etal. (2016).Nanoliposomal irinotecan with fluorouracil and folinicacidin metastatic pancreatic cancer after previous gemcitabine-based therapy (NAPOLI-1): A global, randomised, open-label, phase 3 trial. *Lancet.* 387:545– 557.
46. Ye WL,DuJB,Zhang BL, Na R,Song YF,Mei QB, etal.(2014).Cellular uptake and antitumor activity of PIV-hyd-PEG-FA nanoparticles. *PLoSOne* .9(5):e97358.
47. ZhouJ,ZhaoWY,MaX,JuRJ,LiXY,LiN, etal.(2013).The anticancer efficacy of paclitaxel liposomes modified with mitochondrial targeting conjugate in resistant lung cancer. *Biomaterials.* 34:3626–3638
48. VeroneseFM and MeroA(2008).The Impact of PEGylation on Biological Therapies. *BioDrugs.* 22(5) (2008): 315-329
49. UleryBD,NairLS ,Laurencin CT(2011).Biomedical applications of biodegradable polymers. *J. Polym. Sci. B Polym. Phys.* 49: 832–864.
50. StudentS,HejmoT,Hejmo AP, LeśniakA, BułdakR(2020).Anti-androgen hormonal therapy for cancer and other diseases.*Eur.J. Pharmacol.* 866:172783.
51. RussellSJandBarberGN(2018).Oncolytic virusesasantigen-agnosticcancer vaccines. *Cancer Cell.* 33(4): 599-605.